



Contents lists available at ScienceDirect

## Advanced Powder Technology

journal homepage: [www.elsevier.com/locate/apt](http://www.elsevier.com/locate/apt)

Original Research Paper

## Influence of temperature on the packing dynamics of polymer powders

G. Lumay<sup>a,\*</sup>, F. Francqui<sup>b</sup>, C. Detrembleur<sup>c</sup>, N. Vandewalle<sup>a</sup><sup>a</sup>GRASP Laboratory, CESAM Research Unit, University of Liège, Belgium<sup>b</sup>GranuTools, Awans, Belgium<sup>c</sup>CERM Laboratory, CESAM Research Unit, University of Liège, Belgium

## ARTICLE INFO

## Article history:

Received 30 May 2020

Received in revised form 14 September 2020

Accepted 17 September 2020

Available online xxx

## Keywords:

Polymer powders

Packing dynamics

Temperature

Melting

Caking

## ABSTRACT

Temperature influences drastically the physical properties of polymer powders. In the present study, the packing dynamics of polymer powders has been investigated with a modified version of GranuPack instrument, which is an improvement of the classical tapped density measurement. After the filling procedure, the sample is heated and the evolution of the density is measured after each tap. For a selection of four polymers (polyamide 12, Polystyrene, Polyvinyl chloride and a thermoplastic polyurethane), the influence of temperature on the Hausner ratio and on the packing dynamics are analysed. We show that the packing dynamics is drastically influenced by temperature even far below the melting temperature  $T_m$  for semi-crystalline polymers and far below the glass-transition temperatures  $T_g$  for amorphous polymers. In addition, we show that the analysis of the packing dynamics at different temperatures allows to determine a characteristic temperature corresponding to the onset of caking. Finally, we show that this temperature is coherent with Differential Scanning Calorimetry (DSC) analysis.

© 2020 The Society of Powder Technology Japan. Published by Elsevier B.V. and The Society of Powder Technology Japan. All rights reserved.

## 1. Introduction

Granular materials, fine powders and nanopowders are widely used in industrial applications. However, there are still many challenges to understand their behavior [1–4]. In order to control and to optimize processing methods, these materials have to be precisely characterized [5–7]. This characterization is related either to the properties of the grains (size and shape distribution, roughness, porosity, ...) and to the behavior of the assembly of grains (packing dynamics, flow, agglomeration, segregation, ...). To perform representative measurements, the environmental conditions (temperature and relative humidity) during the measurement should match the conditions in the application.

Powder behavior is influenced by (i) steric repulsion, (ii) friction forces (iii) cohesive forces and (iv) interaction with the surrounding gas. The steric repulsion is related to grain geometry. Friction forces are influenced by both the surface state (rough or smooth surface) and the chemical nature of the grains. Cohesive forces may be induced by the presence of liquid bridges [8–11], by electrostatic charges [12], by van der Waals interactions [13,14] or more rarely by magnetic dipole–dipole interactions [15–18]. The predominance of one of these forces depends on the environmental

conditions. Moisture is known to affect static and dynamic behaviors of granular materials. Indeed, moisture influences both surface grains conductivity and capillary bridges formation. It is also well known empirically that the temperature is affecting the interaction between the grains. Temperature and humidity are also affecting breakage behavior of the grains [20].

The flow properties and the packing dynamics of powders at high temperature is of particular importance for additive manufacturing methods based on selective layer melting, in particular with polymer powder [19,21,22]. The powder is preheated (usually between 40 °C and 90 °C above the glass transition temperature) to decrease the amount of energy needed for the laser irradiation to melt the powder. Therefore, the flowability of the powder must be sufficient at this preheating temperature to produce uniform powder layers during the recoating process. Moreover, the packing density influences the fusing dynamics of the patterned layer and as a consequence the mechanical properties of the printed object. The flowing properties of polymer powders at high temperatures must be also well controlled for extrusion applications [23].

The influence of temperature on polymer powder flow has been investigated very recently with a shear cell [21] and with a custom laboratory device mimicking the recoating process inside a 3D printer [22]. In particular, the shear cell has been used with polyamide 12 from ambient temperature to values close to melting temperature of the polymer [21]. The flowability indexes are found

\* Corresponding author.

E-mail address: [geoffroy.lumay@uliege.be](mailto:geoffroy.lumay@uliege.be) (G. Lumay).

to be relatively constant till 140 °C and increase suddenly at 160 °C. The melting temperature being  $T_m = 180$  °C.

The analysis of a powder sample submitted to successive taps gives information about the packing dynamics and also about powder flowability. Beyond the classical tapped density measurement methods [24], an improved method called GranuPack [7,25] has been developed recently based on fundamental research results [13,17,26–30]. The density of the powder is measured automatically after each tap to obtain a packing curve (also called compaction curve). The analysis of this curve gives classical parameters like bulk and tapped density, Hausner ratio, Carr index but also dynamical parameters (see Section 2.2.1 for additional information). In addition to packing dynamics, this set of parameters characterizes powder flowability.

In the present paper, we show how temperature influences the packing dynamics and as a consequence the flowability of polymer powders by using GranuPack instrument equipped with a heating system. In particular, we show that the temperature influences drastically the packing dynamics far below the melting temperature. Moreover, the analysis of the parameters extracted from packing curves allows to measure the temperature corresponding to the onset of caking. Finally, we show that these temperatures are coherent with Differential Scanning Calorimetry (DSC) measurements.

## 2. Materials and methods

### 2.1. Materials

The aim of the present paper is not to compare commercial powders but to present a new characterisation method particularly suited to studying the influence of temperature on both the flow and the packing dynamics of polymer powders. Therefore, we do not communicate the brandname of the considered samples but we present a detailed description of these powder through granulo-morphometry measurement and differential scanning calorimetry (DSC).

Four polymers have been selected: polyamide 12 (PA12), Polystyrene (PS), Polyvinyl chloride (PVC) and a thermoplastic polyurethane (TPU). The PA12 is a typical powder used in additive manufacturing. Three samples of PS have been considered with different grain sizes. The grain size and shape are analysed in Section 3.1.

### 2.2. Methods

#### 2.2.1. GranuPack high temperature

GranuPack instrument has been recently adapted to perform measurement at high temperature. First, the measurement cell has been equipped with an electrical heating jacket coupled with a thermocouple to measure the temperature of the measurement cell. Second, the inductive sensor used in the classical GranuPack to measure the pile height  $h$  has been replaced by a laser sensor situated farthest from the hot sample. The measurement cell used for the present study was able to heat up the sample till 200 °C. The ambient temperature in the laboratory was  $21$  °C  $\pm$   $2$  °C at a relative humidity of  $35\% \pm 5\%$ .

A volume of powder is placed in a metallic tube with an automated initialization process explained in previous publications [7,25]. This initialisation process is performed at room temperature. Afterward, a light hollow cylinder is placed on top of the powder bed to keep the powder/air interface flat during the packing process and also to play the role of thermal insulator. Then, the cell is heated to the selected temperature and a waiting period of 30 min is applied before starting the tapping. As shown in

Appendix A.1, this waiting time is sufficient to obtain a uniform temperature inside the sample. For each polymer powder, a series of experiments were conducted from ambient to higher temperatures starting always from a new sample at ambient temperature. Moreover, the complete melting of the sample was not investigated (i) to avoid a complex cleaning process of the measurement cell and (ii) to keep focused on the analysis of the system in the granular state.

To perform the taps, the tube containing the powder sample rises up to a height of  $\Delta Z$  and performs free falls. The height  $h$  of the powder bed is measured automatically after each tap with the laser sensor. From the height  $h$ , the volume  $V$  of the pile is computed. As the powder mass  $m$  is known, the density  $\rho$ , which is the ratio between the mass  $m$  and the powder bed volume  $V$ , is evaluated and plotted after each tap to obtain a packing curve. For the present study, the volume of powder was 40 ml, the free fall was fixed to  $\Delta Z = 1$  mm and 500 taps were applied to the sample.

Fig. 1 shows a typical packing curve and the corresponding parameters. The initial density (or bulk density)  $\rho(0) = \rho_0$ , the final density (or tapped density)  $\rho(500) = \rho_{500}$  and the Hausner ratio  $Hr = \rho(500)/\rho(0)$  are the very classical parameters. These parameters are characterizing the range of densities that one could obtain with the powder as a function of its history. In addition, dynamical parameters characterizing the packing speed can be extracted: the number of taps  $n_{1/2}$  needed to reach one half of the packing range and the slope  $\alpha$  at the beginning of the process. As shown by Fig. 1,  $\alpha$  is obtained with the linear fitting  $\rho(n) = \rho_0 + \alpha n$  of the first points. Since this dynamical parameter is measured at the beginning of the packing curve, it is related to the regime with the lowest confinement and the highest mobility of the grains. Therefore, this parameter  $\alpha$  is expected to be related to flowability. Finally, the packing curve can be analysed more deeply by fitting theoretical models (not shown in the present study).

#### 2.2.2. Granulo-Morphometer

The grain size and morphology have been measured with the Occhio 500 Nano high resolution granulo-morphometer from the company Occhio, Belgium. The powder sample was dispersed on a glass plate with the vacuum dispersion system and analysed with a camera.

The central granulometric value (Median  $d(v, 0.5)$ ), the extreme values ( $d(v, 0.9)$  and  $d(v, 0.1)$ ), the distribution width (Span) and the circularity are taken into account in the present study. The averages are performed in volume. The median  $d(v, 0.5)$  is defined as the diameter at which value half of the population volume lies below. Similarly, the extreme values  $d(v, 0.1)$  and  $d(v, 0.9)$  are defined as the diameter at which value 10% and 90% of the population volume lies below. The Span is defined as:

$$\text{Span} = \frac{d(v, 0.9) - d(v, 0.1)}{d(v, 0.5)}. \quad (1)$$

If the distribution is narrow, the Span becomes smaller. Finally the circularity (isoperimetric quotient) is defined as:

$$Q = \frac{4\pi A_p}{c_p^2}, \quad (2)$$

where  $A_p$  is the projected area of the particle image and  $c_p$  is the perimeter calculated by summing the length of the boundary pixels of the particle image. For a perfect circle and by extension sphere  $Q = 1$  and  $Q$  decreases when the particle shape deviates from the spherical shape.

An optical microscope has also been used to observe the grains. The microscope is a Nikon Eclipse FN1 in bright field configuration with an objective 10X.

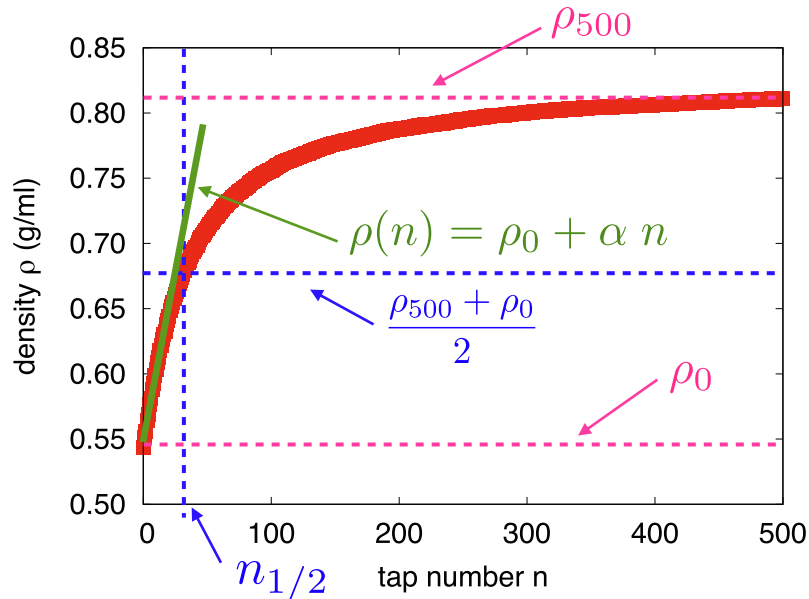


**Fig. 1.** Typical packing curve (also commonly called compaction curve) presenting the density as a function of the tap number. The curve obtained with GranuPack instrument is annotated with the parameters extracted from the curve.

### 2.2.3. DSC

Differential scanning calorimetry (DSC) was performed on a Q1000 TA Instruments calorimeter. The samples were analyzed at a heating rate of  $10\text{ }^{\circ}\text{C min}^{-1}$  over a temperature range from 0 to  $200\text{ }^{\circ}\text{C}$  for PS and PVC, from  $-80\text{ }^{\circ}\text{C}$  to  $200\text{ }^{\circ}\text{C}$  for PA and from  $-80\text{ }^{\circ}\text{C}$  to  $220\text{ }^{\circ}\text{C}$  for TPU under a  $\text{N}_2$  atmosphere. Glass transition temperature ( $T_g$ ) and melting temperature ( $T_m$ ) are determined during the first heating scan in order to take into account the history of the sample and to analyze the sample as received.

## 3. Results

### 3.1. Grain size and morphology

A selection of grain pictures obtained with the Granulomorphometer are presented in Fig. 2. All the PS grains (PS20,

PS80 and PS140) are spherical with only weak imperfections. On the opposite, PA12 and PVC grains are irregular while TPU grains are strongly irregular.

The parameters extracted from the grain size distribution are presented in Table 1. The three PS samples are covering a relatively wide range of median sizes from 22 to  $142\text{ }\mu\text{m}$  to study the influence of grain size. Hereafter, we will compare the results obtained with PS80, PA12, TPU and PVC having median size of the same order of magnitude.

### 3.2. Packing dynamics

Fig. 3 shows the packing curves obtained at different temperatures for a selection of four different powders having relatively similar grain sizes: PA12, PS80, PVC and TPU. The measurement has been repeated three times with PA12 at  $22\text{ }^{\circ}\text{C}$  and  $75\text{ }^{\circ}\text{C}$  and

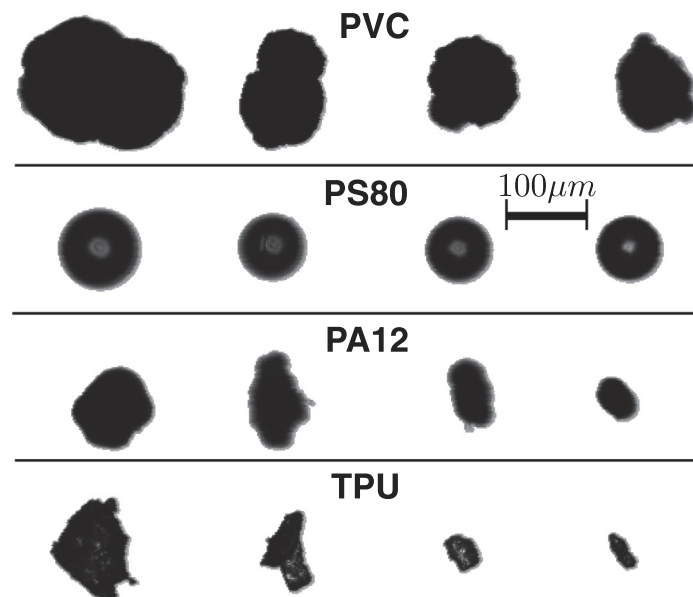


**Fig. 2.** Typical picture of the grains. Only PS80 is presented because PS20 and PS140 have the same spherical shape. To make the comparison easier, the same scale is used for all pictures.

**Table 1**

Main granulometry and morphology indexes: the median diameter  $d(v, 0.5)$ , the extreme values  $d(v, 0.9)$  and  $d(v, 0.1)$ , the distribution width (Span) and the circularity  $Q$ . The sizes are expressed in  $\mu\text{m}$ .

Polymer	$d(v, 0.1)$	$d(v, 0.5)$	$d(v, 0.9)$	Span	$Q$
PVC	84	114	151	0.59	0.85
PS20	20	22	27	0.28	0.89
PS80	78	79	80	0.03	0.88
PS140	141	142	144	0.02	0.90
PA12	45	64	79	0.53	0.84
TPU	25	48	83	1.20	0.74

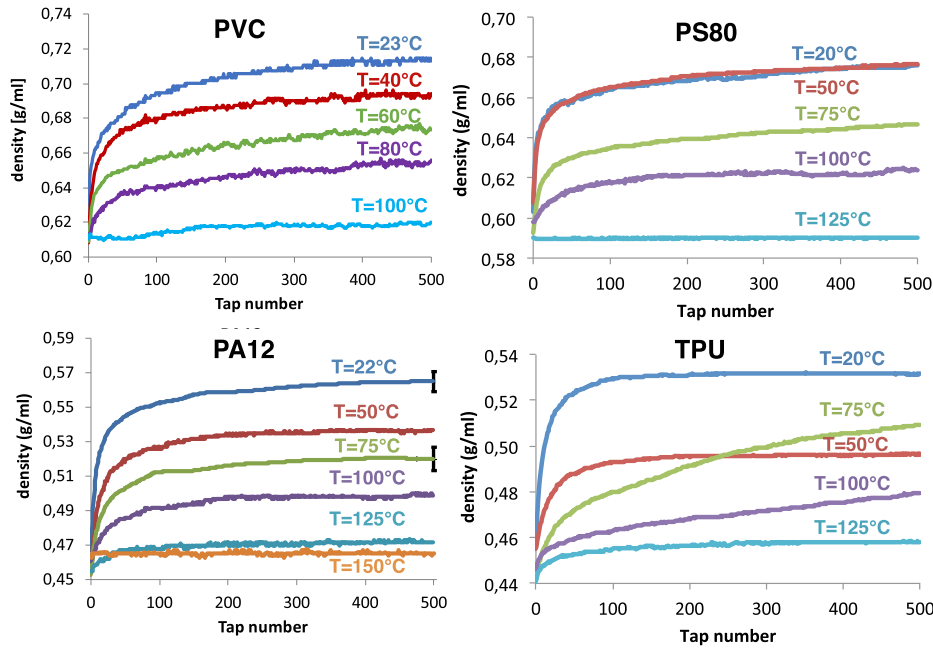


**Fig. 3.** Packing curves obtained with powders PVC, PS80, PA12, and TPU at different temperatures. When the temperature increases, the packing dynamics is slowed down and the final density is reduced, i.e. the packing curve is flattened.

the error bars corresponding to the standard deviation are presented only for the last point. For the same powder, all the curves are starting from the same density  $\rho(0)$  because the initialization is done at room temperature.

The classical way to analyse a tapped density measurement is based on the Hausner ratio  $Hr$  which decreases usually when the flowability increases. In the present configuration, the trend is inverted and  $Hr$  is found to decrease to  $Hr = 1$  when the temperature increases and then when the powder becomes more and more sticky. The decrease of  $Hr$  as a function of the temperature is shown by Fig. 4. The initialisation performed at room temperature to start always from the same initial density  $\rho_0$  explains partially this particular behavior. As shown by Fig. 4 (left) the temperature  $T_{Hr=1}$  corresponding to  $Hr = 1$  depends strongly on the material. Since the temperatures  $T_{Hr=1}$  were approached but not exceeded to avoid a complete melting of the sample (see explanation in Section 2.2.1), an extrapolation is needed to measure this temperature. The evolution of  $Hr$  with the temperature is not necessarily linear and the development of a physical model to fit this trend is an interesting perspective. For the present study, the temperature  $T_{Hr=1}$  has been calculated with a simple linear fit of the three last points. For the set of measurements with the same materials (PS) but with different grain size, the Hausner ratio drops to  $Hr = 1$  roughly at the same temperature (see Fig. 4 (right)). To go further in this analysis, we will focus on the study of the packing dynamics.

The packing speed is also modified by temperature. The characteristic number of taps  $n_{1/2}$  is a good candidate for this characterization. However,  $n_{1/2}$  is converging to infinity when the temperature increases and the measurement of a characteristic temperature is more difficult. Therefore, we selected the other dynamic parameter corresponding to the slope  $\alpha$  of the packing curve during the first taps (see Fig. 1). Fig. 5 shows the decrease of the initial slope  $\alpha$  as a function of the temperature for the different materials (left) and for different grain size (right). As for the temperature  $T_{Hr=1}$  and for the same reasons, the temperature  $T_{\alpha=0}$  corresponding to  $\alpha = 0$  has been calculated with a linear fit of the three last points. This temperature  $T_{\alpha=0}$  depends on the material but less on the grain size and may be considered as the onset of caking. This terminology will be justified hereafter with microscopic observations.

### 3.3. Thermal properties

Table 2 presents the glass-transition temperatures ( $T_g$ ) and melting temperatures ( $T_m$ ) extracted from the DSC curves presented in Fig. 6. In addition, these transition temperatures are compared with the onset of caking characterized by both  $T_{Hr=1}$  and  $T_{\alpha=0}$  measured with GranuPack. For each powders, the temperatures  $T_{Hr=1}$  related to packing range and  $T_{\alpha=0}$  related to packing dynamics are very similar. The error estimation given by the fitting

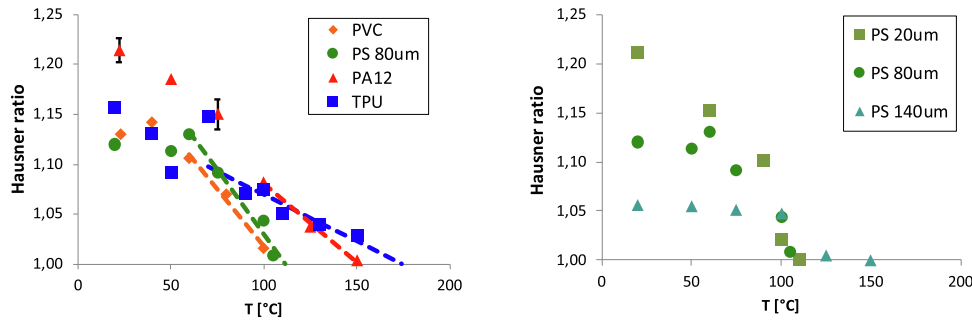


**Fig. 4.** (Left) Evolution of the Hausner ratio  $H_r$  as a function of the temperature for the powders PVC, PS80, PA12 and TPU. The dashed lines are corresponding to linear fits of the last points to obtain the characteristic temperature  $T_{H_r=1}$ . The error bars presented for PA12 at 22 °C and 75 °C are corresponding to the standard deviation computed from three measurements. (Right) Evolution of the Hausner ratio as a function of the temperature for PS powders with different grain sizes.

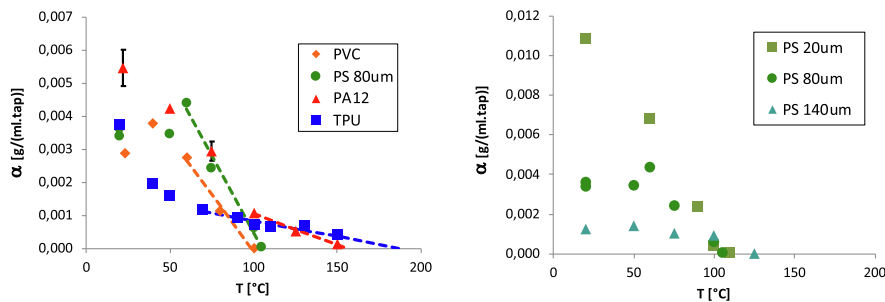


**Fig. 5.** (Left) Evolution of the packing curve initial slope  $\alpha$  as a function of the temperature for the powders PVC, PS80, PA12 and TPU. The dashed lines are corresponding to linear fits of the last points to obtain the characteristic temperature  $T_{\alpha=0}$ . The error bars presented for PA12 at 22 °C and 75 °C are corresponding to the standard deviation computed from three measurements. (Right) Evolution of the slope  $\alpha$  as a function of the temperature for PS powders with different grain sizes.

**Table 2**

Temperatures (expressed in °C) characterizing the set of powders.  $T_g$  and  $T_m$  were measured with DSC from the curves presented in Fig. 6.  $T_{H_r=1}$  and  $T_{\alpha=0}$  have been extracted from GranuPack measurements.

Polymer	DSC		GranuPack	
	$T_g$ (°C)	$T_m$ (°C)	$T_{H_r=1}$ (°C)	$T_{\alpha=0}$ (°C)
PVC	82	amorphous	108	98
PS80	107	amorphous	112	105
PA12	51	185	151	156
TPU	-24	73 and 175	174	187

method used to obtain these temperatures is around 8%. Therefore, one can consider that they are identical.

### 3.4. Microscopic observations

In order to investigate the possible modification of the grain morphology and also to find additional information about the type of interaction between the grains, the state of the powder after a measurement has been analyzed qualitatively and the grains have been observed with an optical microscope. PS80 powder has been selected to perform this analysis because the grains are smooth and spherical, facilitating the observation of morphological modifications. Fig. 7(top) presents pictures of PS80 powder and Fig. 7 (bottom) shows the pictures of the grains obtained with the optical microscope after a measurement at intermediate temperature (75 °C) and at a temperature close to the onset of caking (110 °C). After a measurement at intermediate temperature, the powder contains agglomerates. These agglomerates are highly brittle. According to the observation with the microscope, we do not see any modification of the grains. However, after a measurement at a temperature close to the onset of caking, the powder forms a cake due to the formation of solid bridges between the grains. A

picture of some grains extracted from the cake are shown in Fig. 7(bottom, right). The grains are keeping their spherical shape with dots at their surface at the position of these bridges.

## 4. Discussion

The temperature is found to affect significantly the packing dynamics even at relatively low temperature. When the temperature increases, the range of density variation is reduced and the dynamics is slowed down. The density stays constant when the temperature reaches a critical value. At this critical temperature that we named onset of caking, the polymer chains between the adjacent grains are forming stable bridges between them (necking process). These bridges observed with a microscope (see Fig. 7) are strong enough to survive tapping events. This onset of caking has been quantified with two methods. Firstly by analysing the decrease of the Hausner ratio to  $H_r = 1$  and secondly by analysing the decrease of the initial slope  $\alpha$ , giving respectively the temperatures  $T_{H_r=1}$  and  $T_{\alpha=0}$ . As shown by Table 2, these temperatures are close to each other and the temperature  $T_{\alpha=0}$  will be considered for the rest of the discussion.

The shear cell measurements with polyamide 12 presented in [21] are showing that the flowability indexes are relatively constant till 140 °C and increase suddenly at 160 °C. With the present packing dynamics measurement, a significant effect of the temperature is already observed at 50 °C. We must be careful in the comparison because, even if the grain size and shape are very similar, the powders could be different, in particular due to the presence of additives. However, the packing dynamics measurement is known to be highly sensitive to the cohesive forces between the grains [10,17,30]. In particular, we compared packing dynamics and shear cell measurements for a set of pharmaceutical powders ranging from free-flowing to highly cohesive in [30]. For powders having a low flow factor in the shear cell the dynamical parameters

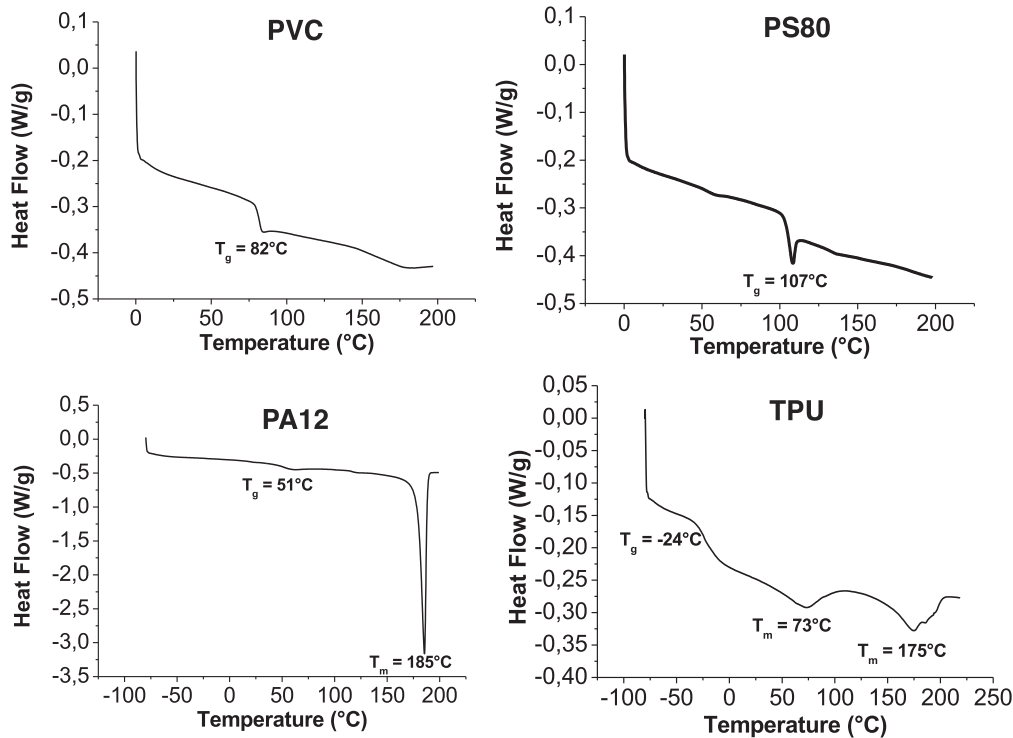


Fig. 6. DSC curves obtained with powders PA12, PS80, PVC and TPU. The temperatures  $T_g$  and  $T_m$  extracted from these curves are summarized in Table 2.

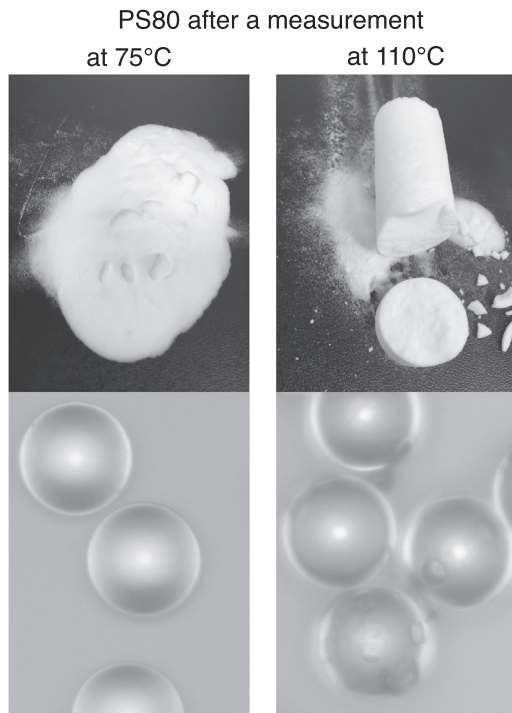


Fig. 7. Pictures of PS80 powder (top) and micrographs of the grains (bottom) after a measurement at 75 °C (left) and 110 °C (right).

obtained from packing measurement are showing a good sensitivity. Therefore, the effect observed at lower temperature with the packing dynamics measurement compared to the shear cell measurement is not surprising.

When comparing DSC results and packing analysis, two distinct cases are observed depending on the nature of the polymer, i.e.

whether it is amorphous or semi-crystalline. For the amorphous ones (PS80 and PVC), the onset of caking (determined by  $T_{\alpha=0}$ ) is expected to occur when the polymer chains are mobile and thus flowing, therefore when the polymer is approaching its  $T_g$ . Then,  $T_{\alpha=0}$  is almost identical to the  $T_g$  of the polymers. For PVC,  $T_{\alpha=0}$  is slightly higher but in the same range. For the semi-crystalline polymers (PA12 and TPU), the  $T_m$  values are determined at the apex of the endothermic peak. While PA presents a quite sharp  $T_m$  at 185 °C, TPU presents two very broad  $T_m$  around 73 °C and 175 °C, certainly due to the presence of two types of crystallites. These broad  $T_m$  indicate that these crystallites are starting to melt well before this temperature and are completely molten well after (about 30 °C after the measured  $T_m$ ). For these semi-crystalline polymers, the onset of caking  $T_{\alpha=0}$  is much higher than  $T_g$  and close to  $T_m$  (the second one for TPU). Indeed, at a temperature between  $T_g$  and  $T_m$ , the polymer chains are not free to flow. Although the amorphous part of the chains have some mobility, the chains are still “linked” to their non-molten crystalline regions [31–33]. When the crystallites are melting (at  $T_m$ ), the polymer chains are free to flow, leading to the onset of caking. Therefore  $T_{\alpha=0}$  values are close to the highest  $T_m$  for semi-crystalline polymers. Note that the melting of the crystallites is occurring over a rather large temperature range, which might explain why  $T_{\alpha=0}$  is close but not identical to  $T_m$ .

Among the set of polymers considered in the present study, TPU shows a particular behavior. Indeed, TPU polymers are complex materials with multi-domain structure (hard and soft regions). The packing curves obtained with TPU at intermediate temperatures (see TPU curve at 75 °C in Fig. 3) are showing a second increase which is certainly due to the particular elastic and thermal properties of this material. As shown by Fig. 6, the DSC curve is also showing a peak at 73 °C with TPU. The onset of caking  $T_{\alpha=0}$  corresponds to the second  $T_m$  at 176 °C and the particular packing behavior corresponds to the first  $T_m$  at 73 °C. Moreover, comparing to the other materials, the decrease of the initial slope  $\alpha$  with temperature is particularly non linear with TPU (see Fig. 5 (left)). The decrease is

fast for low temperature and slows down when approaching the onset of caking. This transition between the fast and slow decrease is also around 70 °C, i.e. close to the first  $T_m$  at 73 °C.

An increase of the temperature can modify the different forces of interaction between the grains through different mechanisms. The Young modulus of the polymer decreases with temperature [34], increasing the surface of contacts and therefore the friction force. With polymers, cohesive/adhesive forces are also expected to increase with temperature [35]. Obviously, when approaching or reaching the melting temperature of the material forming the grains, the melting at the contact between the grains will modify the interactions and also possibly the shape of the grains. In the present study concerning polymer powders, we assume that these are the main mechanisms influencing the packing dynamics.

In powders containing moisture, a modification of the temperature will modify the water thermodynamic equilibrium inside the powder and induce a set of complex mechanisms. The capillary bridges could evaporate creating possibly solid bridges, the water contained inside the grains could migrate to the surface, the water could experience vaporisation, etc. An important effect of moisture is not expected with the polymer powders considered in the present study but the systematic study of these effects with food or pharmaceutical powders for example is a stimulating perspective.

We have shown in previous studies [27,28] that the packing dynamics is governed by the mobility of the grains. This mobility is reduced when friction or cohesive forces become stronger. The packing dynamics is therefore slowed down leading to a decrease of the slope  $\alpha$ . Moreover, the increase of the inter-grain forces with temperature reduces the ability of the grains to find configurations optimizing the density. Therefore, the Hausner ratio decreases also with temperature.

## 5. Conclusion

Overall, the effect of temperature on the packing dynamics of polymer powder is strong. In particular, the packing dynamics is significantly modified even at low temperature compared to melting temperature  $T_m$  for semi-crystalline polymers and to glass-transition temperatures  $T_g$  for amorphous polymers. Therefore, the packing dynamics measurement is a good candidate to quantify the effect of the temperature on polymer powders and is found to be more sensitive than the shear cell methods at low temperature.

From the packing curves obtained at different temperatures and for different polymer powders, the classical Hausner ratio characterizing the density modification and the initial slope characteriz-

ing the packing dynamics have been extracted. Both parameters are decreasing with temperature do reach unity for Hausner ratio and to converge to zero for the initial slope allowing to measure two characteristic temperatures  $T_{Hr=1}$  and  $T_{\alpha=0}$ . These two temperatures are close and are characterizing the onset of caking induced by the formation of stable bridges between adjacent grains.

A particular packing behavior has been evidenced with TPU powder at 75 °C and confirmed by DSC measurements showing a second  $T_m$  at 73 °C. Therefore, the packing dynamics measurement is also able to predict particular thermal properties of powders.

A systematic study of the effect of temperature on the packing dynamics with other families of powders (food, pharmaceutical, metal, ceramic powders) is a stimulating perspective. Moreover, the packing dynamics measurement is a promising method from both fundamental and applied perspectives. From a fundamental perspective, the development of physical models taking the different forces between the grains into account to fit the data could allow to identify the most pertinent physical parameters and mechanisms. From an applied or industrial perspective, the packing dynamics analysis at different temperatures is a characterization method that makes sense in additive manufacturing for example.

## Declaration of Competing Interest

The authors declare that they have no known competing financial interests or personal relationships that could have appeared to influence the work reported in this paper.

## Acknowledgments

C.D. is FNRS Research Director and thanks FNRS for financial support and Charlotte Dannemark for the DSC analysis. We thank Naveen Tripathi and Aurelien Neveu from GranuTools for their support.

## Appendix A

### A.1. Temperature uniformity

To check the temperature uniformity in the sample and also the time needed to reach the final temperature, four small thermocouples have been positioned inside the powder sample (PA12) and one thermocouple was following the temperature of the tube. Inside the powder sample, the thermocouples were positioned in the center of the tube at different heights from the bottom of the

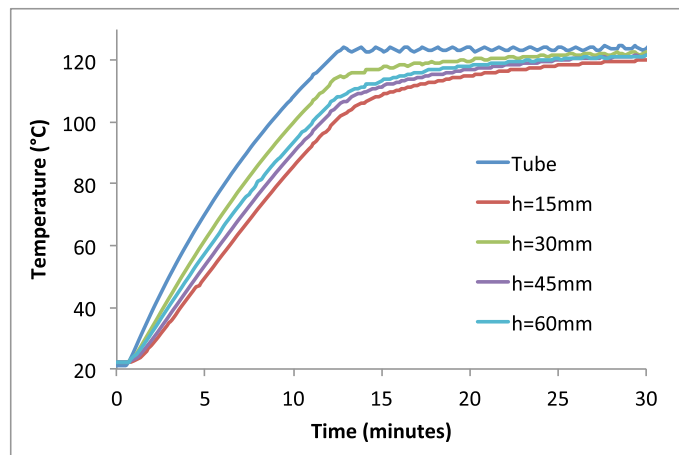


Fig. A.8. Temporal evolution of the temperature at different heights in the powder sample and of the tube.

cell (15 mm, 30 mm, 45 mm and 60 mm). The powder height was 80 mm. The temporal evolution of the temperatures is shown in Fig. A.8. The final temperature was set to 125 °C.

## References

- [1] P.G. de Gennes, Granular matter: a tentative view, *Rev. Mod. Phys.* 71 (1999) S374.
- [2] H.M. Jaeger, S.R. Nagel, Physics of the Granular State, *Science* 255 (1992) 1524.
- [3] G.D.R. MiDi, On dense granular flows, *Eur. Phys. J. E* 14 (2004) 341.
- [4] B. Andreotti, Y. Forterre, O. Pouliquen, *Granular Media: Between Fluid and Solid*, Cambridge University Press, 2013.
- [5] D. Geldart, E.C. Abdullah, A. Verlinden, Characterisation of dry powders, *Powder Technol.* 190 (2009) 70.
- [6] M. Krantz, H. Zhang, J. Zhu, Characterization of powder flow: Static and dynamic testing, *Powder Technol.* 194 (2009) 239.
- [7] G. Lumay, F. Boschini, K. Traina, S. Bontempi, J.-C. Remy, R. Cloots, N. Vandewalle, Measuring the flowing properties of powders and grains, *Powder Technol.* 224 (2012) 19.
- [8] G. Landi, D. Barletta, M. Poletto, Modelling and experiments on the effect of air humidity on the flow properties of glass powders, *Powder Technol.* 207 (2011) 437.
- [9] A. Kudrolli, Granular Matter - Sticky Sand, *Nat. Mater.* 7 (2008) 174.
- [10] J.E. Fiscina, G. Lumay, F. Ludewig, N. Vandewalle, Compaction dynamics of wet granular assemblies, *Phys. Rev. Lett.* 105 (2010) 048001.
- [11] E. Emery, J. Oliver, T. Pugsley, J. Sharma, J. Zhou, Flowability of moist pharmaceutical powders, *Powder Technol.* 189 (2009) 409.
- [12] E. Mersch, G. Lumay, F. Boschini, N. Vandewalle, Effect of an electric field on an intermittent granular flow, *Phys. Rev. E* 81 (2010) 041309.
- [13] J.M. Valverde, A. Castellanos, Random loose packing of cohesive granular materials, *Europhys. Lett.* 75 (2006) 985.
- [14] A. Castellanos, J.M.V., A.T. Perez, A. Ramos, P.K. Watson, Flow regimes in fine cohesive powders, *Phys. Rev. Lett.*, 82 (1999) 1156.
- [15] J.M. Valverde, M.J. Espin, M.A.S. Quintanilla, A. Castellanos, Magnetofluidization of fine magnetite powder, *Phys. Rev. E* 79 (2009) 031306.
- [16] G. Lumay, N. Vandewalle, Controlled flow of smart powders, *Phys. Rev. E* 78 (2008) 061302.
- [17] G. Lumay, S. Dorbolo, N. Vandewalle, Compaction dynamics of a magnetized powder, *Phys. Rev. E* 80 (2009) 041302.
- [18] G. Lumay, N. Vandewalle, Flow of magnetized grains in a rotating drum, *Phys. Rev. E* 82 (2010) 040301.
- [19] S.C. Ligon, R. Liska, J. Stampfl, M. Gurr, R. Mulhaupt, Polymers for 3D printing and customized additive manufacturing, *Chem. Rev.* 117 (2017) 10212–10290.
- [20] D. Olusanmi, C. Wang, M. Ghadiri, Y. Ding, K.J. Roberts, Effect of temperature and humidity on the breakage behaviour of Aspirin and sucrose particles, *Powder Technol.* 201 (2010) 248.
- [21] D. Ruggi, C. Barres, J.-Y. Charneau, R. Fulchiron, D. Barletta, M. Poletto, A quantitative approach to assess high temperature flow properties of a PA 12 powder for laser sintering, *Additive Manuf.* 33 (2020) 101143.
- [22] M. Van den Eynde, L. Verbelen, P. Van Puyvelde, Influence of temperature on the flowability of polymer powders in laser sintering, *AIP Conf. Proc.* 1914 (2017) 190007.
- [23] F. Desplentere, S. Deceur, M. Vandaele, Advanced rheological characterisation for thermal sensitive materials using shear heating device, *AIP Conf. Proc.* 2107 (2019) 040002.
- [24] European pharmacopoeia 7.0, Chapter 2.9.36.: Powder flow, p. 308.
- [25] K. Traina, R. Cloots, S. Bontempi, G. Lumay, N. Vandewalle, F. Boschini, Flow abilities of powders and granular materials evidenced from dynamical tap density measurement, *Powder Technol.* 235 (2013) 842–852.
- [26] G. Lumay, N. Vandewalle, Compaction of anisotropic granular materials: Experiments and simulations, *Phys. Rev. E* 70 (2004) 051314.
- [27] G. Lumay, N. Vandewalle, Experimental study of granular compaction dynamics at different scales: grain mobility, hexagonal domains, and packing fraction, *Phys. Rev. Lett.* 95 (2005) 028002.
- [28] G. Lumay, N. Vandewalle, Experimental study of the compaction dynamics for two-dimensional anisotropic granular materials, *Phys. Rev. E* 74 (2006) 021301.
- [29] P. Richard, M. Nicodemi, R. Delannay, P. Ribi re, D. Bideau, Slow relaxation and compaction of granular systems, *Nat. Mater.* 4 (2005) 121.
- [30] G. Lumay, N. Vandewalle, C. Bodson, L. Delattre, O. Gerasimov, Linking compaction dynamics to the flow properties of powders, *Appl. Phys. Lett.* 89 (2006) 093505.
- [31] J.E. Mark, A. Eisenberg, W.W. Graessley, L. Mandelkern, J.L. Koenig, Physical properties of polymers, *Am. Chem. Soc.* (1984) 55–95.
- [32] G.W. Ehrenstein, R.P. Thieriault, *Polymeric Materials: Structure, Properties, Applications*, Springer, 2001, pp. 67–78.
- [33] A.J. Peacock, A. Calhoun, *Polymer Chemistry, Properties and applications*, Carl Hanser Verlag, 2006, pp. 67–78.
- [34] G.V. Salmoria, J.L. Leite, L.F. Vieira, A.T.N. Pires, C.R.M. Roesler, Mechanical properties of PA6/PA12 blend specimens prepared by selective laser sintering, *Polym. Testing* 31 (2012).
- [35] B. Cappella, W. Stark, Adhesion of amorphous polymers as a function of temperature probed with AFM force–distance curves, *J. Colloid Interface Sci.* 296 (2006) 0021.